Journal of Alloys and Compounds 509 (2011) L348–L351

Contents lists available at ScienceDirect

Journal of Alloys and Compounds

journal homepage: www.elsevier.com/locate/jallcom

Letter

Synthesis and luminescence properties of clew-like $CaMoO_4$:Sm^{3+}, Eu^{3+}

Ye Jin [a,*], Jiahua Zhang [b,*], Zhendong Hao [b], Xia Zhang [b], Xiao-jun Wang [b,c]

[a] Department of Applied Physics, School of Optoelectronic Information, Chongqing University of Technology, 69 Hongguang Street, Chongqing 400054,China
[b] Key Laboratory of Excited State Processes, Changchun Institute of Optics, Fine Mechanics and Physics, Chinese Academy of Sciences, 16 Eastern South Lake Road, Changchun 130033, China
[c] Department of Physics, Georgia Southern University, Statesboro, Georgia 30460, USA

ARTICLE INFO

Article history:
Received 23 April 2011
Received in revised form 14 July 2011
Accepted 15 July 2011
Available online 22 July 2011

Keywords:
Luminescence
Microclew
$CaMoO_4$:Sm^{3+}
Eu^{3+}
Energy transfer

ABSTRACT

Eu^{3+} and Sm^{3+} co-doped $CaMoO_4$ microclews have been successfully synthesized via a facile hydrothermal method directly in surfactant-free environment. The as-prepared phosphor present clew-like agglomerates composed of 40 nm nanosheets under the moderated reaction temperature. The red phosphor $CaMoO_4$:Eu^{3+}, Sm^{3+} can generate a strong absorption line at 405 nm, originating from $^6H_{5/2} \rightarrow {}^6P_{5/2}$ transition of Sm^{3+}, which is suitable for the emission of the near-ultraviolet light-emitting diodes (~400 nm). Energy transfer between Sm^{3+} and Eu^{3+} is detected from the varied photoluminescence spectra with different Eu^{3+} concentrations and the energy transfer mechanism is clarified via the photoluminescence spectra. When Sm^{3+} is excited (405 nm), the electron is excited from $^6H_{5/2}$ to $^6P_{5/2}$, and then relaxed to $^4G_{5/2}$. It jumps from $^4G_{5/2}$ to the lower levels corresponding to the emissions of Sm^{3+}; meanwhile, the transfers from $^4G_{5/2}$ state of Sm^{3+} ion to $^5D_0$ state of Eu^{3+} ion come out. The transition of $^5D_1 \rightarrow {}^7F_J$ (J = 0, 1, 2) does not appear indicating that the transfer from $^4G_{5/2}$ state of Sm^{3+} to $^5D_0$ state rather than $^5D_1$ state of Eu^{3+} is the energy transfer pathway.

1. Introduction

The luminescence properties of nano-phosphor receive much attention, because it is significant not only for applications but also for essential understanding of nanocrystals, such as confinement effect, surface effect, etc. [1–5]. Recently, rare earth doped phosphors for white-light-emitting diodes (W-LEDs) have received increasing interest because the promising applications of LED on illuminations with advantages over the existing incandescent and halogen lamps in power efficiency, reliability, long lifetime and environmental protection [6–9]. Eu^{3+} doped $CaMoO_4$ has been investigated extensively as a red-emitting phosphor for near-ultraviolet (UV) GaN chip (350–420 nm) based W-LEDs, due to the less stable property of current red phosphor material Y_2O_2S [10]. Other ions are introduced into $CaMoO_4$:Eu^{3+} to enhance the luminescence intensity, such as Bi^{3+}, Sm^{3+} [11,12]. The introduction of Sm^{3+} into $CaMoO_4$:Eu^{3+} can generate a strong excitation line at 405 nm, originating from $^6H_{5/2} \rightarrow {}^4K_{11/2}$ transition of Sm^{3+}, which is suitable for the excitation of the UV-LED.

Energy transfer plays a crucial role in luminescent materials and the luminescence intensities are also various with the co-doped ions due to the existence of the energy transfer. Rare earth ions, such as Eu^{2+}, Ce^{3+} ions etc., often acts as efficient sensitizers that transfer energy to other ions like Mn^{2+}, Tb^{3+} in several host lattices [13–15]. The energy transfer from Ce^{3+} to Tb^{3+} is greatly investigated in a commercially applied lamp phosphor $LaPO_4$:Ce^{3+}, Tb^{3+} with high emission yields, up to 93% [16–18]. Recently, Hong investigated the energy transfer property in Eu^{2+} and Ce^{3+} co-doped $SrCaSiO_4$ and revealed that the co-doping of Ce^{3+} enhanced the emission intensity of Eu^{2+} greatly [19]. Energy transfer from Sm^{3+} to Eu^{3+} is also confirmed in $NaEu(MoO_4)_2$ [20,21] and other molybdate [22]. However, the bidirectional energy transfer between Eu^{3+} ions and Sm^{3+} ions and the corresponding energy transfer pathway have not been investigated in detail. Accordingly in this article, it is reported that the energy transfer property between Eu^{3+} ions and Sm^{3+} ions in clew-like $CaMoO_4$ microstructure composed of nanosheets which is directly synthesized by a facile hydrothermal method without surfactant. The energy transfer pathway is proved sufficiently to be between $^4G_{5/2}$ state of Sm^{3+} ions and $^5D_0$ state, rather than $^5D_1$ state of Eu^{3+}.

2. Experimental

All the raw chemical materials were used without further purification. The clew-like $CaMoO_4$ was synthesized via a facile hydrothermal method. Na_2MoO_4 solution and $Ca(NO_3)_2$ solution with appreciated proportion $Eu(NO_3)_3$ (0.1 M) or $Sm(NO_3)_3$ (0.01 M) were prepared respectively. The Na_2MoO_4 solution was poured into $Ca(NO_3)_2$:Eu^{3+}, Sm^{3+} solution under vigorously stirring. A white precipitate was immediately observed in the glass beaker and the pH value of the solution was stabilized at an appropriate constant. The vigorously stirring was kept for 30 min. Then,

* Corresponding authors. Tel.: +86 023 62563051.
E-mail addresses: jinye3446@yahoo.com.cn (Y. Jin), jinye3446@yahoo.com.cn (J. Zhang).

0925-8388/$ – see front matter © 2011 Elsevier B.V. All rights reserved.
doi:10.1016/j.jallcom.2011.07.047

the precursor solution was transferred into a 50 mL Teflon-lined stainless steel autoclave, which was subsequently sealed and maintained at 140 °C for 8 h. After that, the autoclave was allowed to cool down to room temperature naturally. The product was filtered and washed several times with deionized water and absolute ethanol. It is followed that the product was dried in the air at around 100 °C for 2 h. Finally, white powder of Sm^{3+} ions and Eu^{3+} ions co-doped clew-like $CaMoO_4$ was ready for further characterization.

The structures of samples were characterized by X-ray diffraction (XRD) (Rigaku D/max-rA powder diffractometer with Cu target radiation resource (λ = 1.54078 Å)). The morphology was investigated by using field emission scanning electron microscopy (FE-SEM) (Hitachi S-4800). Fluorescence and excitation spectra were recorded at room temperature using a Hitachi F-4500 spectrophotometer equipped with a 150 W Xe-arc lamp. The emission spectra of all samples were measured at a fixed band-pass of 0.2 nm with the same instrument parameters.

3. Results and discussion

The structure of the as-prepared clew-like $CaMoO_4$ was determined by XRD. As shown in Fig. 1, all of the diffraction peaks for the $CaMoO_4$:1 mol% Sm^{3+} can be ascribed to the tetragonal structure $CaMoO_4$, consistent with the standard data file (JCPDS No.85-0585). No other peaks can be found in the patterns indicating that the dopant ions didn't change the structure of hosts.

As shown in Fig. 2a, a typical low-magnification SEM image indicates that the as-synthesized products consist of a large quantity of 3D microstructure. The clewlike microstructures have diameters of 5 μm and thickness up to 2.5 μm. A representative medium-magnification SEM image of several $CaMoO_4$:Eu^{3+}, Sm^{3+} clews, as shown in Fig. 2b and c, reveals that their clew-like shape with a hole at the central of the 3D microstructure, which is distinct from other previous reported $CaMoO_4$: RE nano- or microstructures [23]. Fig. 2d shows a high-magnification SEM image of some clewlike $CaMoO_4$:Eu^{3+}, Sm^{3+}, indicating that the 3D microclew is consisted of 40 nm-thickness nanoflakes.

Fig. 3 shows the emission (λ_{ex} = 405 nm) and excitation (λ_{em} = 595 nm) spectra of clewlike CaMoO4: *x*% Sm^{3+} (*x* = 0.1–5). The excitation spectra (Fig. 3a) for monitoring the $^4G_{5/2} \rightarrow {}^6H_{7/2}$

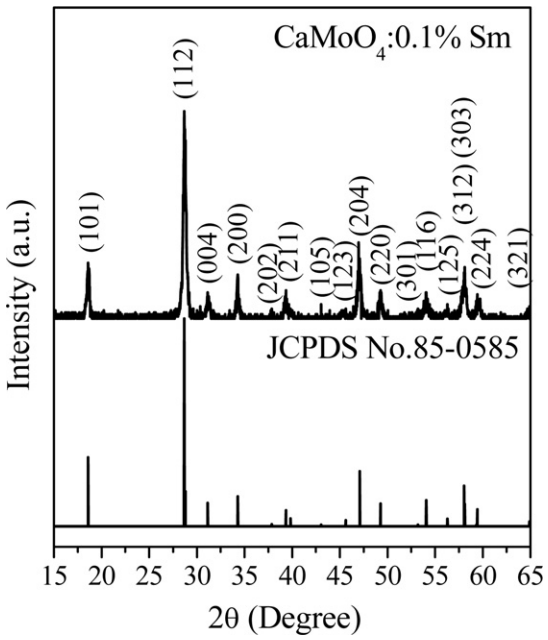

Fig. 1. XRD patterns for $CaMoO_4$: 0.1% Sm^{3+}.

emission at 595 nm of Sm^{3+} show a broad band in the range of 200–300 nm assigned to the charge transfer transition of MoO_4^{2-} with some sharp lines in the range of 340–450 nm corresponding to the f-f transitions of Sm^{3+} ions (the enlarger in the inset of Fig. 3a) [24], mainly including $^6H_{5/2} \rightarrow {}^4K_{11/2}$ transition at 405 nm. Under 405 nm excitation, the products emit reddish orange light and the emission spectra were recorded, as shown in Fig. 3b. The emission spectra exhibit three characteristic transitions of Sm^{3+}, $^4G_{5/2} \rightarrow {}^6H_{5/2}$, $^4G_{5/2} \rightarrow {}^6H_{7/2}$ and $^4G_{5/2} \rightarrow {}^6H_{9/2}$. The dependence

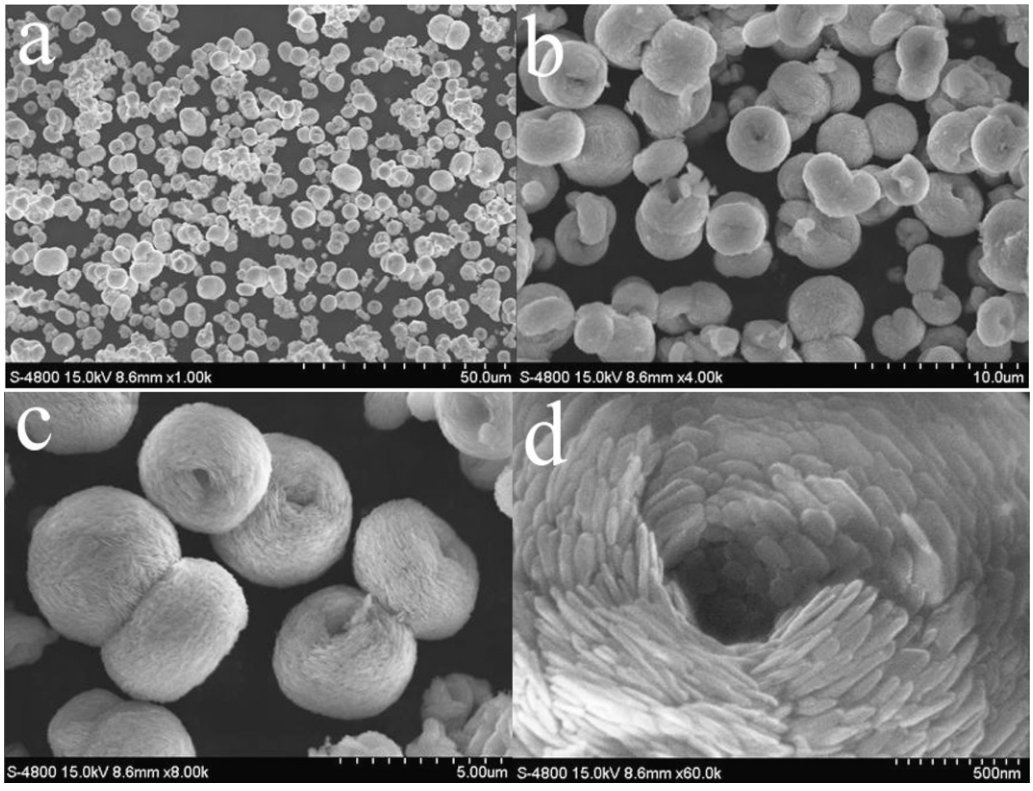

Fig. 2. SEM images of the $CaMoO_4$:Eu^{3+}, Sm^{3+}: (a) low magnification; (b) and (c) medium magnification; (d) high magnification.

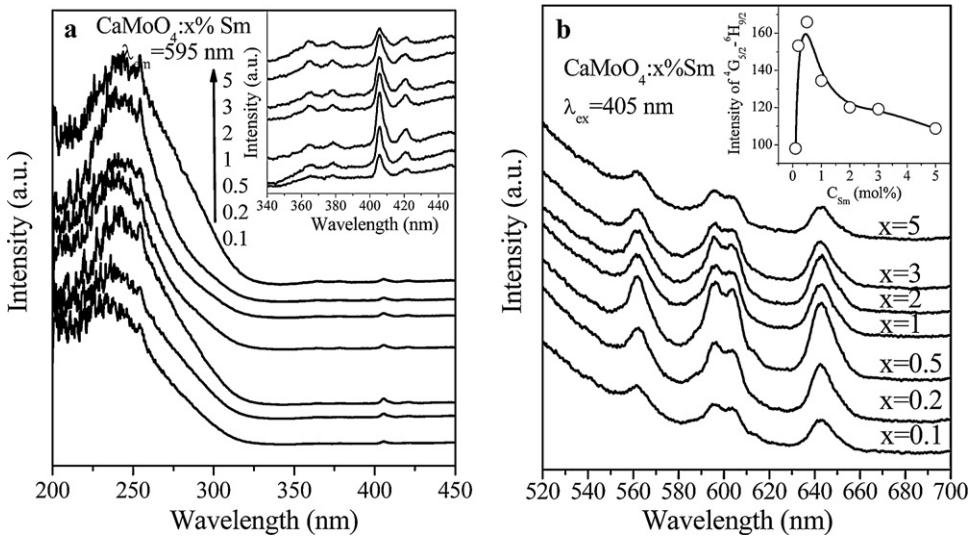

Fig. 3. Excitation (a) (λ_{em} = 595 nm) and emission (b) (λ_{ex} = 405 nm) spectra of clewlike $CaMoO_4$: *x*% Sm^{3+} (*x* = 0.1–5).

of the integrated emission intensity on Sm^{3+}concentration is presented in the insert of Fig. 3b, which demonstrates the optimal Sm^{3+} concentration of 0.5% in $CaMoO_4$. In the following experiment, the concentration of Sm^{3+} is, hence, fixed at 0.5%.

The emission spectra of $CaMoO_4$:Eu^{3+}, $CaMoO_4$:Sm^{3+} and $CaMoO_4$:Eu^{3+}, Sm^{3+} are shown in Fig. 4 for comparison. The emission spectrum of $CaMoO_4$:Eu^{3+} under 395 nm excitation, shown in Fig. 4a, consists of lines ranging from 500 to 700 nm that come from the transitions of $^5D_{0,1}$ to ^7F_J (J = 1, 2, 3, 4, not in all cases) levels of the Eu^{3+} activators. The most intense emission is the $^5D_0$–$^7F_2$ transition in the range of 600–620 nm, located at the red area. The emission spectrum of $CaMoO_4$:Sm^{3+} (λ_{ex} = 405 nm) shows the typical emissions corresponding to the transitions from the $^4G_{5/2}$ level to $^6H_{5/2}$, $^6H_{7/2}$, and $^6H_{5/2}$ levels, respectively (Fig. 4b). Both of these two samples emit red light under UV light irradiation. As shown in Fig. 4c, under 405 nm excitation into the $^4K_{11/2}$ level of Sm^{3+} in Eu^{3+} and Sm^{3+} co-doped sample, the characteristic emissions of Eu^{3+} are also noticeable, indicating the energy transfers from Sm^{3+} to Eu^{3+}.

Fig. 5 depicts the photoluminescence excitation spectra of Sm^{3+} singly doped $CaMoO_4$ and Eu^{3+} and Sm^{3+} co-doped $CaMoO_4$. In the Sm^{3+} singly doped $CaMoO_4$, the excitation spectrum monitoring 561 nm is composed of a series of narrow peaks attributed to the f–f transition of Sm^{3+}. In the Eu^{3+} and Sm^{3+} co-doped sample, the excitation spectrum monitoring at 612 nm of Eu^{3+} appears the $^6H_{5/2} \rightarrow {}^4K_{11/2}$ transition of Sm^{3+} at 405 nm (Fig. 5b), and that monitoring at 561 nm of Sm^{3+} appears the $^7F_0$–$^5L_6$ transition of Eu^{3+} at 395 nm (Fig. 5c). This indicates bidirectional energy transfer between Sm^{3+} and Eu^{3+} in $CaMoO_4$.

The emission spectra of Eu^{3+} and Sm^{3+} co-doped $CaMoO_4$ under different pump wavelength were measured and are shown in Fig. 6. As shown in Fig. 6a, under 270 nm excitation, all the characteristic emissions of Eu^{3+} and Sm^{3+} can be observed, displaying the energy transfer form the broad charge transfer band (CTB) of O–Mo. The emission at 533 nm corresponding to $^5D_1 \rightarrow {}^7F_0$ ($<20 \times 10^3$ cm^{-1}) transition of Eu^{3+} can be observed when the sample was excited under 270 nm (Fig. 6a) and 395 nm excitation (Fig. 6b). However, under 405 nm excitation, it disappears while the emission

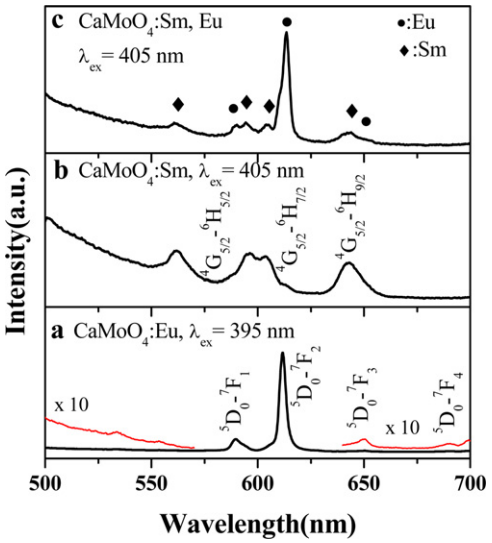

Fig. 4. Emission spectra of $CaMoO_4$:Eu^{3+} (a) (λ_{ex} = 395 nm), $CaMoO_4$:Sm^{3+} (b) (λ_{ex} = 405 nm), $CaMoO_4$:Eu^{3+}, Sm^{3+} (c) (λ_{ex} = 405 nm).

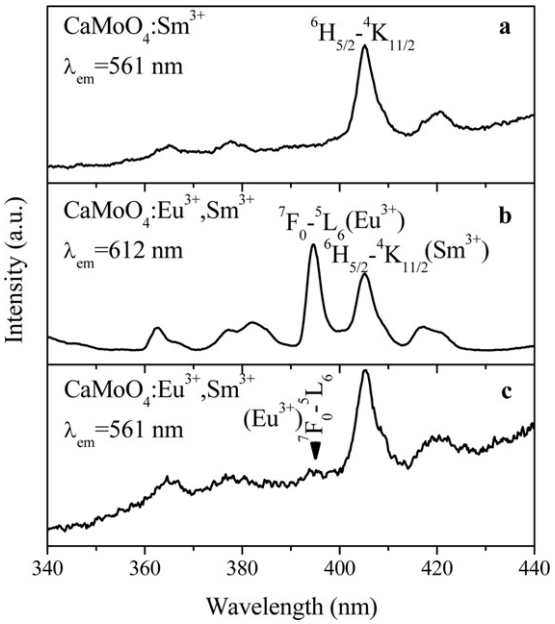

Fig. 5. Photoluminescence excitation spectra of $CaMoO_4$: Sm^{3+} (a) (λ_{em} = 561 nm), $CaMoO_4$: Eu^{3+}, Sm^{3+} (b) (λ_{em} = 612 nm), $CaMoO_4$:Eu^{3+}, Sm^{3+} (c) (λ_{em} = 561 nm).

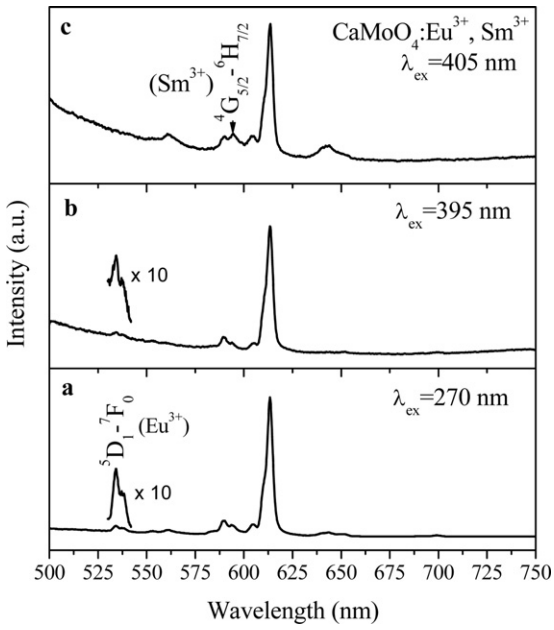

Fig. 6. Emission spectra of $CaMoO_4$: Eu^{3+}, Sm^{3+} (a: λ_{ex} = 270 nm, b: λ_{ex} = 395 nm, c: λ_{ex} = 405 nm).

corresponding to $^4G_{5/2} \rightarrow {}^6H_{7/2}$ transition of Sm^{3+} is enhanced (Fig. 6c). Due to the other transitions from $^5D_0$ level of Eu^{3+} are still be observed, the electron is considered to be transferred from $^4K_{11/2}$ state of Sm^{3+} to $^5D_0$ state, rather than $^5D_1$ state of Eu^{3+}.

4. Conclusions

In conclusion, the clew-like $CaMoO_4$:Eu^{3+}, Sm^{3+} microstructure which is consisted of nanosheets has been synthesized by using facile hydrothermal method without surfactant. The bidirectional energy transfer between Eu^{3+} ions and Sm^{3+} ions has been detected by photoluminescence spectra. And the transfer processes is discussed, namely, the energy transfer occurs between $^4G_{5/2}$ state of Sm^{3+} ions and $^5D_0$ state rather than $^5D_1$ state of Eu^{3+} ions. This result is quite remarkable for the furthermore investigation on the Eu^{3+} and Sm^{3+} co-doped materials.

Acknowledgment

This work is financially supported by the National Nature Science Foundation of China (10834006, 10774141, 10904141, and 10904140), the Scientific Project of Jilin province (20090134, 20090524) and CAS Innovation Program, the Youth Foundation of Chongqing University of Technology (2011ZQ21).

References

[1] T. Takagahara, K. Takeda, Phys. Rev. B 46 (1992) 15578.
[2] F. Bødker, S. Mørup, S. Linderoth, Phys. Rev. Lett. 72 (1994) 282.
[3] W.F. Peng, S.Y. Zou, G.X. Liu, Q.L. Xiao, R. Zhang, L.J. Xie, L.W. Cao, J.X. Meng, Y.L. Liu, J. Alloys Compd. 509 (2011) 6673.
[4] G. Jia, C. Zhang, L. Wang, S. Ding, H. You, J. Alloys Compd. 509 (2011) 6418.
[5] Z.H. Li, J.H. Zeng, Y.D. Li, Small 3 (2007) 438.
[6] W. Lü, Z.D. Hao, X. Zhang, Y.S. Luo, X.X. Wang, J.H. Zhang, J. Lumin. 131 (2011) 2387.
[7] D.K. Williams, B. Bihari, B.M. Tissue, J.M. McHale, J. Phys. Chem. B 102 (1998) 916.
[8] A. Setlur, E. Radkov, C. Henderson, J. Her, A. Srivastava, N. Karkada, M. Kishore, N. Kumar, D. Aesram, A. Deshoande, B. Kolodin, L. Grigorov, U. Happek, Chem. Mater. 22 (2010) 4076.
[9] N. Hirosaki, R.J. Xie, K. Kimoto, T. Sekiguchi, Y. Yamamoto, T. Suehiro, M. Mitomo, Appl. Phys. Lett. 86 (2005) 211905.
[10] Z.L. Wang, H.B. Liang, J. Wang, M.L. Gong, Q. Su, Appl. Phys. Lett. 89 (2006) 071921.
[11] S.X. Yan, J.H. Zhang, X. Zhang, S.Z. Lu, X.G. Ren, Z.G. Nie, X.J. Wang, J. Phys. Chem. C 111 (2007) 13256.
[12] Y. Jin, J.H. Zhang, S.Z. Lu, H.F. Zhao, X. Zhang, X.J. Wang, J. Phys. Chem. C 112 (2008) 5860.
[13] U.G. Caldino, A.F. Munoz, J.O. Rubio, J. Phys.: Condens. Matter 2 (1990) 6071.
[14] G.Q. Yao, J.H. Lin, L. Zhang, G.X. Lu, M.L. Gong, M.Z. Su, J. Mater. Chem. 8 (1998) 585.
[15] W.J. Yang, L.Y. Luo, T.M. Chen, N.S. Wang, Chem. Mater. 17 (2005) 3883.
[16] R.C. Ropp, J. Electrochem, Soc. Solid State Sci. 115 (1968) 841.
[17] J.C. Bourcet, F.K. Kong, J. Chem. Phys. 60 (1974) 34.
[18] B.M.J. Smets, Mater. Chem. Phys. 16 (1987) 283.
[19] H. Yu, Y. Lai, G. Gao, L. Kong, G. Li, S. Gan, G. Hong, J. Alloys Compd. 509 (2011) 6635.
[20] Z.L. Wang, H.B. Liang, M.L. Gong, Q. Su, Electrochem. Solid-State Lett. 8 (2005) H33.
[21] Z.L. Wang, H.B. Liang, M.L. Gong, Q. Su, Opt. Mater. 29 (2007) 896.
[22] X.X. Wang, Y.L. Xian, G. Wang, J.X. Shi, Q. Su, M.L. Gong, Opt. Mater. 30 (2007) 521.
[23] S. Yu, Z.B. Lin, L.Z. Zhang, G.F. Wang, Cryst. Growth Des. 7 (2007) 2397.
[24] S. Shigeo, M.Y. William, Phosphor handbook, CRC Press, 1999, p204.